Tr. J. of Physics
22 (1998) , 645 – 660.

International Workshop on Linac-Ring
Type ep and γp Colliders

A proposal for a measurement of the nucleon form factors at an asymmetric e^+e^- linac-ring collider.

R. BALDINI
Laboratori Nazionali di Frascati dell'INFN, Frascati - ITALY
C. BINI
Universitá "La Sapienza" and INFN Sezione di Roma-1, Roma - ITALY
P. PATTERI*
Laboratori Nazionali di Frascati dell'INFN, Frascati - ITALY

Abstract

The neutron electromagnetic form factors have been measured for the first time in the time-like region in the Q^2 range between 3.6 and 6 GeV^2 by the FENICE experiment. The results show some unexpected features. First the neutron magnetic form factor turns out to be larger than the proton one, the neutron electric form factor being negligible. Then there are indications of a narrow structure very near the $N\overline{N}$ threshold, in the e^+e^-multihadronic annihilation.

A new, high statistics experiment is needed to clarify the indications. An asymmetric, unconventional, linac-storage ring collider is proposed, using one of the existing high energy storage ring for positrons and a few hundred MeV linac for electrons. Advantages of this configuration are outlined and a very conservative evaluation of the luminosity that can be achieved is reported.

1. The nucleon time-like form factors

The nucleon structure can be explored for space-like transfer momentum Q^2 by means of lepton-nucleon interaction and for time-like Q^2 by means of $e^+e^- \to N\bar{N}$ annihilations (in the following Q^2 is defined to be positive in the time-like region). In the space-like region the differential cross section for eN elastic scattering, in the one photon approximation is usually given by the well known Rosenbluth formula [1, 2], where two functions of the square of the transferred momentum Q^2 are introduced to take into account the electromagnetic structure of the nucleon: the Dirac form factor F_1^N and the Pauli form factor F_2^N. A more convenient representation is obtained with the Sachs form factors, defined as

$$G_E^N = F_1^N + \frac{Q^2}{4m^2} F_2^N$$

*Corresponding author, e-mail:bini@vxrm70.roma1.infn.it

$$G_M^N = F_1^N + F_2^N.$$

In the time-like region the connection between the e^+e^-cross sections (total and differential) and the Sachs electromagnetic form factors is given by (α is the fine structure constant, m_N the neutron mass, β the nucleon velocity and θ the angle between the antineutron and the beam direction in the c.m. system) :

$$\sigma = \frac{4\pi\alpha^2\beta}{3s}\left[|G_M|^2 + \frac{2m_N^2}{s}|G_E|^2\right] \tag{1}$$

$$\frac{d\sigma}{d\Omega} = \frac{\alpha^2\beta}{4s}\left[|G_M|^2(1+cos^2\theta) + \frac{4m_N^2}{s}|G_E|^2 sin^2\theta\right] \tag{2}$$

In the time-like region, G_E and G_M are assumed to be the analytical continuation of the space-like form factors. Assuming that also the Dirac and Pauli form factors are analytical throught the $N\overline{N}$ threshold it must be that at $Q^2 = 4m_N^2$, G_E and G_M are equal, i.e. there is the S wave only.

To extract the form factors from the cross section measurement, one needs to know the relative magnitude of $|G_E|$ and $|G_M|$ and in principle this is possible by looking at the angular distribution of the detected events (see relation 2).

In figure 1 the proton time-like magnetic form factor measurements are shown[3, 4] [5]. The magnetic form factor has been extracted under the hypothesis $G_M = G_E$ (theoretically supported only at threshold). According to this hypothesis, the proton angular distribution is expected to be flat near threshold and this is consistent with the present experimental finding in the whole energy range shown in Figure 1a.

The first unexpected feature of the proton time-like form factor in figure 1a is the steep trend very near threshold, suggesting the tail of a quite narrow structure below threshold.

Concerning the general trend, analyticity[6] and PQCD [7] expect that asymptotically the nucleon time-like form factors (magnetic and electric, for proton and neutron) are real and almost equal to the space-like one at the same $|Q^2|$. Furthermore asymptotically the nucleon magnetic form factors must scale as $1/Q^4$.

The proton time-like data are consistent with the $1/Q^4$ behaviour already above $Q^2\sim$ 4 GeV^2 as shown in Figure 1b, but they exceed the space-like data at the same $|Q^2|$ by a factor of 2 [8].

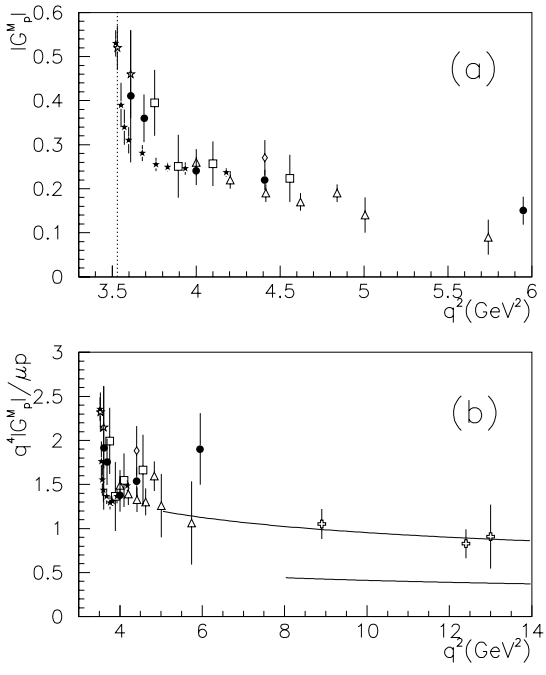

Figure 1. Data on proton time-like form-factors: (a) Low q^2 data; (b) all data multiplied by q^4 fitted with a dipole function for q^2 larger than 5 GeV^2 (solid line) and compared with the level reached by space-like data at the same q^2 (dashed line)

2. Final results from the FENICE experiment

No measurements of the neutron form factors had been performed before FENICE (DM2 had a very poor detection efficiency and, at most, they found 2 candidate events at $Q^2 = 5.75\ GeV^2$).

To measure for the first time the electromagnetic form factor of the neutron in the time like-region the storage ring ADONE was restored as e^+e^-collider in 1990. ADONE operated in a single bunch mode at c.m. energies from 1.8 to 3.1 GeV, with $\sim 10^{29} cm^{-2} s^{-1}$ peak luminosity.

The FENICE detector is described in detail elsewhere[9]. Due to the low detection efficiency of a low energy neutron, antineutron detection was chosen as the only signature for the $e^+e^- \to n\bar{n}$ events. The antineutrons were detected by means of the charged products of their annihilation on nuclei and by the measurement of the time of flight with respect to the beam crossing time [10]. It was also possible to identify $p\bar{p}$ and multihadronic events. [4, 11]

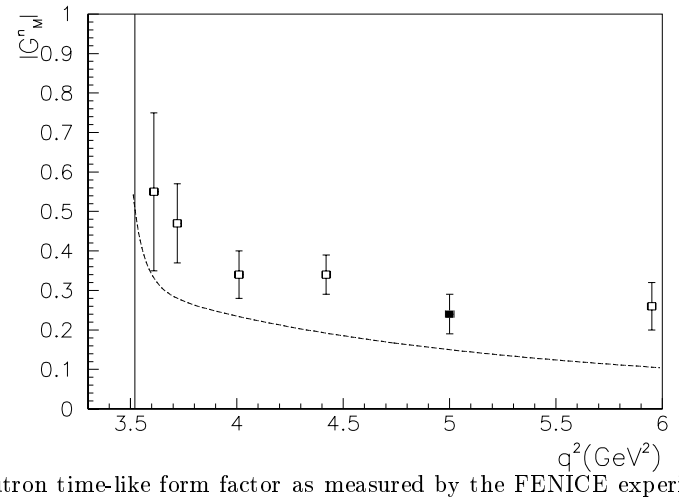

Figure 2. Neutron time-like form factor as measured by the FENICE experiment. Data are extracted in the $|G_E| = 0$ hypothesys. The full square is a measurement by DM2 and a prediction according U-spin conservation, derived by the DM2 Λ form factor measurement[12]. A parametrization of the proton data behaviour of Figure 1(a) is also shown for comparison (dashed curve).

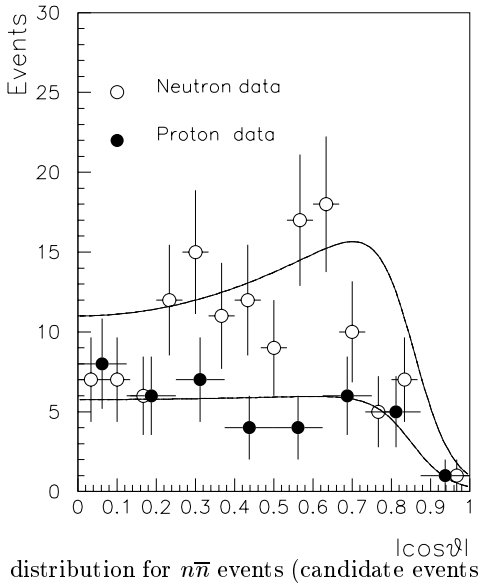

Figure 3. Polar angle θ distribution for $n\overline{n}$ events (candidate events of all the energies) and for $p\overline{p}$ events. The curves superimposed are the fits described.

In Figure 2 the FENICE results on the neutron time-like magnetic form factor are shown. The values of G_M^n have been obtained under the hypothesis $G_E^n/G_M^n \sim 0$. In fact opposite to the proton case, the neutron angular distribution (see Figure 3) is in

agreement with a negligible electric form factor (G_E^n/G_M^n less than 10 % with 90 % confidence level) while $G_E^p \sim G_M^p$ better accounts for the proton data. This indication is in agreement with the aforementioned prejudice of some symmetry between space-like and time-like (at $Q^2 \sim$ -4 GeV^2 it has been measured $G_E^n/G_M^n \sim 0$ [13]).

We notice that the assumption $G_E = G_M$ exactly at threshold demands a neutron magnetic form factor also very small at threshold. Therefore there should be a steep positive derivative of the neutron magnetic form factor, in the same energy range where the proton magnetic form factor has shown the opposite trend.

Analyticity and PQCD expect that time-like and space-like form factors are similar, as mentioned before. Hence the neutron magnetic form factor should be quite smaller than the proton one. More exactly PQCD expects [14] [15] that the ratio between neutron and proton magnetic form factor should be $\sim q_d/q_u = -0.5$. On the contrary, according to FENICE this ratio results

$$G_M^n/G_M^p > 1.$$

That is quite unexpected in any nucleon picture based on quarks. In fact, according to valence quark charges and magnetic moments, the proton is anyhow expected to have larger electromagnetic interactions than the neutron.

The results of the total multihadronic cross section in the Q^2 range $3 \div 5$ GeV^2 as measured by FENICE and by previous experiments at ADONE and DCI [11] are shown in Figure 4.

In the region around the $N\bar{N}$ threshold (dotted line in the figure) there is an indication for a narrow structure. We have considered the hypothesys of the existence of a narrow resonance just below threshold strongly coupled to the $N\overline{N}$ final states and also interfering with the multihadronic amplitude [16, 17]. A combined fit of the multi-hadronic data and the proton form factor data, gives for the resonance an energy of W $\sim$ 1870 MeV with a width $\sim$ 15 MeV.

In conclusion these results strongly suggest:

- anomalous e.m. interactions of the neutron.
- a narrow structure near $N\bar{N}$ threshold;

However, these conclusions are supported by only two experiments, FENICE at ADONE and PS-170 at LEAR, and a new measurement is strongly needed to confirm or dismiss them.

3. An asymmetric e^+e^-collider, using an existing, high energy e^+ storage ring and an e^- linear accelerator

For the FENICE experiment ADONE delivered few times $10^{28} cm^{-2} s^{-1}$ as a mean luminosity and about 500 nb^{-1} integrated luminosity. Therefore a $\sim 10^{30} cm^{-2} s^{-1}$ average luminosity at least is needed, in order to get a real improvement.

ADONE was dismounted in 1993 and the energy range of DAΦNE, the new Φ factory built in the same building, will not reach the $n\bar{n}$ threshold. Other e^+e^-colliders cannot afford at present this luminosity at the $N\bar{N}$ threshold.

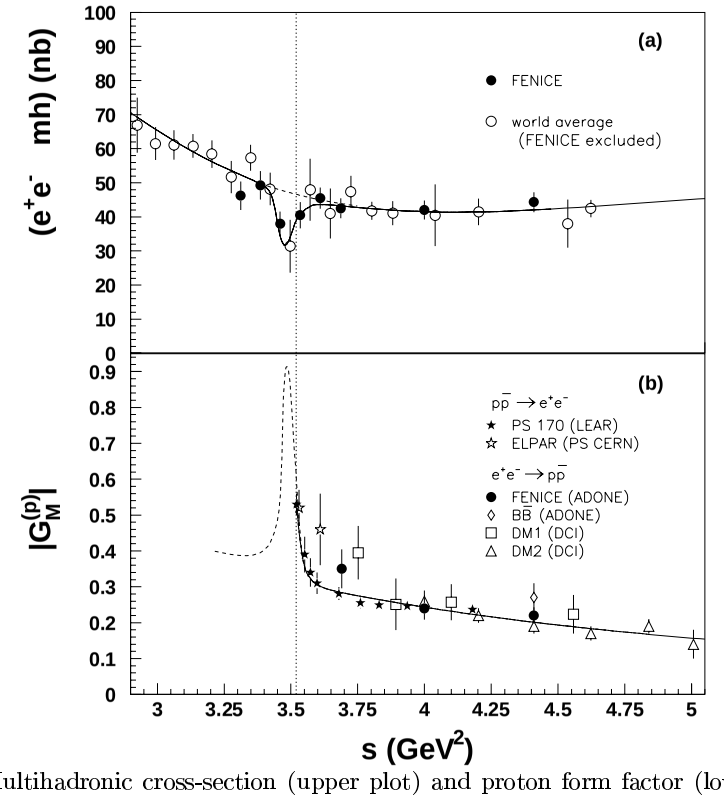

Figure 4. Multihadronic cross-section (upper plot) and proton form factor (lower plot) as a function of the center of mass energy. A combined fit is also shown.

On the other hand, with such a luminosity and with an experimental apparatus having at least 50% detection efficiency, few months integrated luminosity would be enough to get a measurement of the nucleon form factors and of the total multihadronic cross section an order of magnitude better than it is at present.

Furthermore, if transversely polarized beams are available , G_E and G_M can be identified not only by looking to the θ angular distribution, but also by means of the very different ϕ angular distribution.

The experimental apparatus is supposed to identify at the same time nucleon-antinucleon pairs and multihadronic events; with a good luminosity it should be possible to include also accurate measurements near the further thresholds for baryon pair production, in order to check the background and to look for eventual structures.

Last but not least a good measurements of the total multihadronic cross section in the energy range to be explored are barely needed to interpret $\alpha(M_Z^2)$ and the new g_μ-2

very accurate measurements. In fact it has been shown [18] that at present the scanty data in the e^+e^-multihadronic cross section in this energy range are among the main error sources.

We propose to perform the outlined measurements at an asymmetric e^+e^-collider, using an existing high energy e^+ storage ring in the $4 \div 10$ GeV energy region and an e^- linear accelerator (linac) of hundreds MeV energy.

We show first (Sect.4) how the peculiar kinematical condition of the experiment allows to perform a particularly accurate form factor measurement with appreciable advantages respect to the asymmetric configuration; then we present (Sects.5-6) preliminary results of a realistic evaluation of the luminosity achievable exploiting the know-how coming from the TESLA Test Facility e^- superconducting linear accelerator, and using the CESR collider as positron beam. Finally Sect.7 shows possible improvements to this scheme.

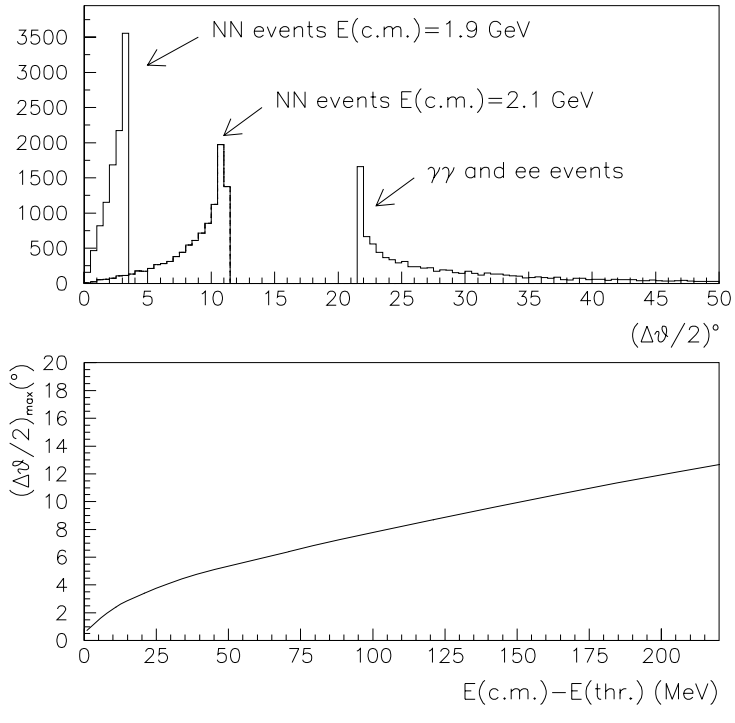

Figure 5. Upper plot: distribution of the half opening angle of the forward cone for $N\overline{N}$ events at two c.m. energies and for low mass particles pairs. Lower plot: half opening angle of $N\overline{N}$ events as a function of the c.m. energy respect to the threshold energy.

4. Some hints for the detector

In the asymmetric e^+e^- configuration the laboratory reference system does not coincide with the c.m. one, hence the particles in the final states will be boosted in the forward direction according to their velocities and angles in the c.m. system.

We have simulated collisions between a 5 GeV circulating positron beam and an electron linac with energy in the $150 \div 250$ MeV range and we have studied the kinematical configuration in the lab system. The results give the following hints in view of a possible detector design.

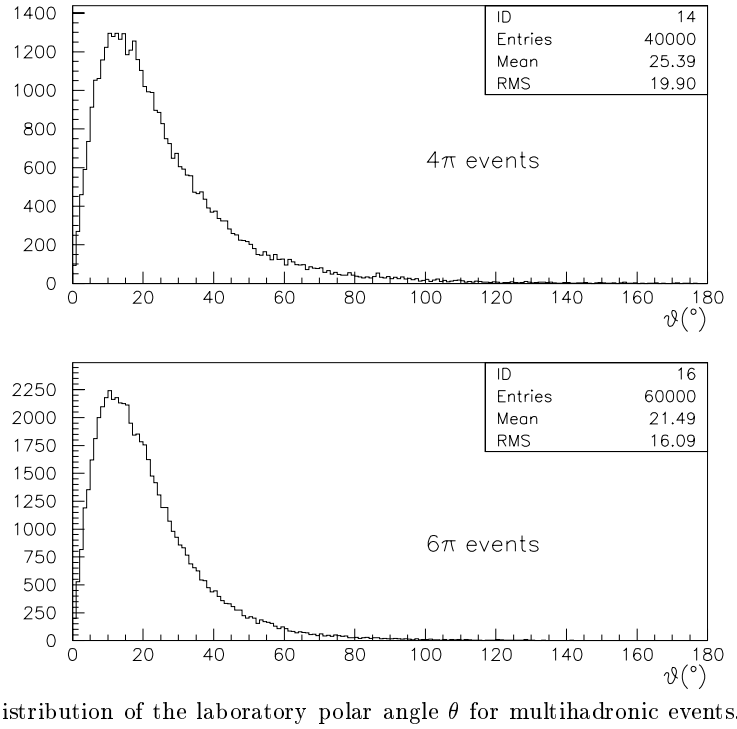

Figure 6. Distribution of the laboratory polar angle θ for multihadronic events. $e^+e^- \to 4\pi$ (upper plot) and $e^+e^- \to 6\pi$ (lower plot).

- The nucleons and the antinucleons, produced nearly at rest in the c.m. reference system, get essentially half of the positron beam energy from the boost so that they can be detected as hadronic showers of the order of few GeV energy. Both particels in the final state can be detected with high efficiency, and a double coincidence could be easily asked for, hence reducing appreciably any conceivable background.
- $N\overline{N}$ pairs are emitted in the lab system within a forward cone (as shown in Figure 5), characterized by a sharp maximum opening angle that, at a given positron beam energy, depends on the center of mass energy. A detector covering the angular range

between 2^0 and $\sim 15^0$ allows to study the full Q^2 range of interest from $10 MeV$ above threshold up to the Strange Baryons threshold.

By the way we notice that for a given center of mass energy, a measurement of the maximum opening angle $(\Delta\theta/2)_{max}$ with an accuracy of the order of ~ 1 mm at 10 m, can give the value of the center of mass energy down to ~ 1 MeV accuracy, that is better than the machine energy scale uncertainty.

- Any other 2-body final state with lower mass (e^+e^-, $\mu^+\mu^-$ $\pi^+\pi^-$ and $\gamma\gamma$) is characterized by a minimum opening angle of the pair (see Figure 5) of $\sim 20^o$, smoothly depending on the energy. Therefore the request of a double coincidence for a nucleon-antinucleon pair, is free from other 2-body final states possible backgrounds.

- The nucleon velocity in the laboratory system is such that, on a base of ~ 10 m, a time of flight difference of ~ 1 ns is expected between nucleons and photons or electrons (coming for instance from beam-gas or beam-pipe interactions); this provides a further discrimination method.

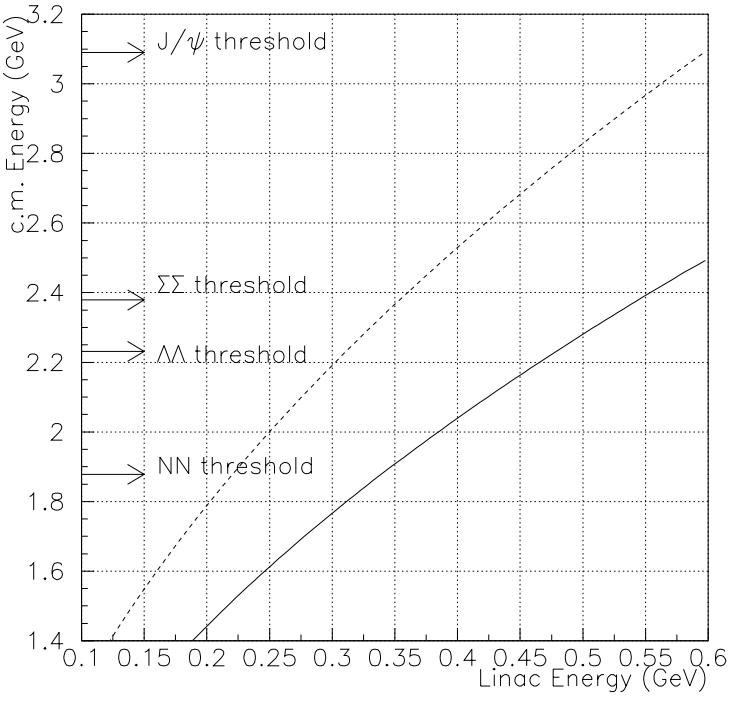

Figure 7. Span of electron energy E_e for head-on collision with positron beam of energy $E_P = 5.3\,GeV$ (continuos line) and $E_P = 8.0\,GeV$ (dashed line) in the invariant mass range between the $n\bar{n}$ threshold and $\sqrt{s} = 3.1\,GeV$. The thresholds for nucleon-antinucleon (nn), $\Lambda\overline{\Lambda}$ (LL), $\Sigma\overline{\Sigma}$ (SS) and J/ψ production are also shown.

The experimental apparatus to detect $e^+e^- \to n\bar{n}$ and $e^+e^- \to p\bar{p}$ (nucleon detector) may be placed several meters far from the interaction region in the forward direction and can be built symmetrically around the beam-pipe. Quadrupoles and bending magnets must be avoided as much as possible along nucleon and antinucleon flight paths. The nucleon detector should consist of a tracking device and of a hadronic calorimeter. The hadron calorimeter should be able to give also a good time of flight measurement.

A toroidal air-core magnet [19] surrounding the beam pipe can be included in order to allow momentum measurements of charged particles without disturbing the beams. Furthermore the present technology allows for few percent radiation length [19], being almost transparent to neutral particles.

As mentioned already the experimental apparatus is supposed to measure at the same time both the $N\overline{N}$ final states and multihadronic events. Figure 6 shows the expected angular distributions in the lab system for 4π and 6π final states generated according to pure phase-space in the c.m. system for the 5 GeV + 200 MeV configuration. It is clear that in order to have a reasonable efficiency for multihadronic events, further tracking devices must be put around the interaction region at least covering all the forward half-space ($0 < \theta < 90^o$). These detectors will also detect large opening angle electron pairs (Bhabha scattering) for luminosity measurement.

In conclusion, the kinematical configuration involved in an e^+e^- asymmetric collider turns out to provide quite relevant advantages, concerning the measurement of nucleon form factors, and easily allows also an accurate measurement of multihadronic cross-sections.

5. A linac ring-collider using CESR

This section presents a preliminary estimate of the luminosity achievable in the c.m. energy range from $1.8\,GeV$ ($\sim N\bar{N}$ threshold) up to $3.1\,GeV$ with an asymmetric e^+e^- collider using CESR.

In the following it is assumed that the positron beam is stored in the ring with energy $E_p = 5.3\,GeV$. The electron beam is provided by a linac or a race-track microtron with energy in the corresponding range $E_e \approx 150 \div 450\,MeV$, it is brought to an interaction point near or inside the ring and then spent in a beam dump far from the interaction region.

The spacing of the e^- bunches must be the same of the e^+ bunches stored in the ring, so that each e^+ bunch collides with one or more bunches in the linac macropulse. This implies the frequencies of the rf system of the machines are armonically related and phase-locked.

The suitable linac energy range to span the energy range $N\bar{N} < \sqrt{s} < J/\psi$ in head-on collision is given by

$$E_e = s/4E_p.$$

The energies corresponding to $N\bar{N}$, $\Lambda\bar{\Lambda}$ and $\Sigma\bar{\Sigma}$ pair thresholds and to J/ψ are also

shown in Figure 7. Dashed line shows the required linac energy range if the ring energy would be raised to $8\,GeV$.

We assume for a preliminary estimate that both beams have transverse gaussian distribution and comparable emittance ϵ, so that the transverse beam sizes can be matched. The linac beam envelope, due to the larger freedom in designing optical function design and lower energy, is shaped to match the stored beam size at the IP.

The luminosity is given by

$$\mathcal{L}[cm^{-2}s^{-1}] = \frac{n_e n_p f_c}{4\pi\sigma_x\sigma_z}$$

where

$$\begin{cases} n_e & = \text{number of electrons in each bunch} \\ n_p & = \text{number of positrons in each bunch} \\ f_c & = \text{bunch collision frequency [Hz]} \\ \sigma_{x(z)} & = \text{rms beam size [cm] at the IP in the x (z) plane.} \end{cases}$$

In both machines the beam sizes are proportional to $\sqrt{\epsilon}$. The dependence of the emittance on the energy is quite different: in a ring $\epsilon^{(SR)} \propto E_p^2$, on the contrary in a linac $\epsilon^{(L)} \propto E_e^{-1}$. Moreover, in a linac horizontal and vertical emittances are nearly equal, meanwhile in a ring the vertical emittance is lower by a factor $0.01 < k < 1$, according to the coupling between radial and vertical plane.

In this first estimate of the achievable luminosity we aimed mainly to defining the minimal performances that the electron accelerator has to provide, so we decided to evaluate the luminosity in a frozen machine configuration. This operating mode [20] has higher n_p with respect to more up to date configurations and is better suited to a linac ring collider since it exploits at the best the limited corrent providable by a linac. A parameter list is shown in Table 1.

According to the parameters in table 1 the CESR vertical emittance at $5.3\,GeV$ varies between $\epsilon^{(SR)} = 1.7 \cdot 10^{-7}\,m\,rad$ at full coupling between radial and vertical planes and $\epsilon^{(SR)} = 5 \cdot 10^{-9}\,m\,rad$ out of coupling, therefore the required linac emittance must be $\epsilon^{(L)} \approx 1 \cdot 10^{-8}\,m\,rad$ @ $200\,MeV$. A linac in a typical injection chain to a storage ring usually cannot provide such a high quality beam, but these performances are commonly achieved in the FEL facilities by the linacs specially equipped with a low emittance gun in the first stage. If the ring is operated at the emittance as low as possible , a very high quality beam would be required; this can be provided only by the best injectors developped for the linear collider test facilities or UV-FEL experiments.

Assuming a fixed ring energy $E_p = 5.3$ or $8.0\,GeV$, the dependence of the linac beam sizes as a function of the c.m. energy $\sqrt{s}$ is given by

$$\sigma_i = 2\sqrt{\frac{\epsilon_L \beta_i E_p}{s}}$$

In order to have constant σ the optical function β must be changed so that β/s is kept constant. That implies at the J/ψ it is $\beta \sim 2.7$ times larger than at the $n\bar{n}$ threshold. Therefore substantial adjustment of the transport line optics must be foreseen when changing the c.m. energy. The parameters referring to the electron beam are based on experimental data or design specifications at the TESLA Test Facility at DESY [21]. These values are comparable with the performances achievable by industrial grade sc technology (see for instance the CEBAF project for a FEL based industrial application of sc technology [22]), so they are a reliable basis for the estimate of the collider performances.

Table 1. Parameter list of the CESR.

Machine parameter		value	unit	Note
Energy	E_p	5.3	GeV	
Orbit length	l_{orb}	768.43	m	
Emittance	ϵ_x^{SR}	$1.2 \cdot 10^{-8}$	$m \cdot rad$	@ 1.0 GeV
Emittance	ϵ_z^{SR}	$1.8 \cdot 10^{-10}$	$m \cdot rad$	@ 1.0 GeV
Radial-vertical coupling	k	0.015		
Particles/bunch	n_p	$2.5 \cdot 10^{11}$		112 mA/7 bunches
Bunch length	σ_y	17	mm	
Bunch spacing	s_b	300	ns	
Horiz. optical function	β_x	1.0	m	
Vert. optical function	β_x	$18 \cdot 10^{-3}$	m	
Beam size	σ_x	574	μm	
Beam size	σ_z	10	μm	
Damping time	τ_x, τ_z	26.9	ms	
Damping time synchr.	τ_s	13.4	ms	

The Tesla Test Facility linac is a 500 MeV superconducting linac under construction at DESY [21], as a test for technological and accelerator physics issues to be investigated looking for the 500 GeV c.m. linear collider TESLA. Its design performances have been specified to study linear collider issues and UV FEL, so are very indicative of the beam quality achievable at the state of art in this field. A parameter set for a superconducting linac suited for collision with the CESR operating according to the parameters in table 1 have been derived and listed in Table 2.

The luminosity attainable with a TTF-like linac beam matching as far as possible the CESR parameters in table 1 is $\mathcal{L} \sim 2 \cdot 10^{29}\, cm^{-2} s^{-1}$.

This value can be improved when considering different time distribution of the linac and ring current; of course, injector and power plant must be capable of providing a different time structure.

The maximum linac current limits $qn_e \cdot f_b = I_m < 8\, mA$. However, a reduction of linac pulse frequency implies a corresponding increase in the number of particles per bunch at constant current both in the ring and linac beam, so that $\mathcal{L} \propto f_b^{-1}$. The corresponding luminosity as a function of the number of bunches stored in the ring is shown in Figure 8.

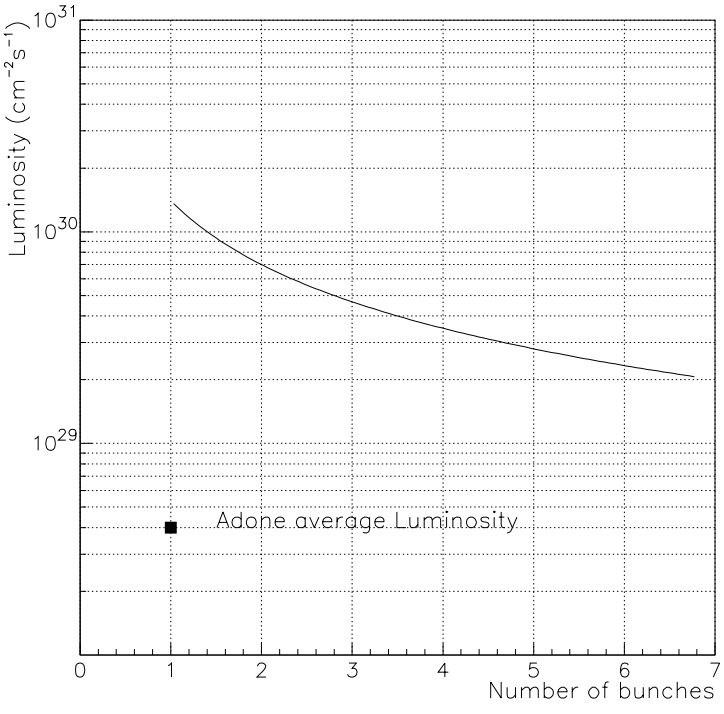

Figure 8. Luminosity vs. number of stored bunches in CESR at 112 mA. The average luminosity achieved at ADONE for the FENICE experiment is shown for comparison.

The single bunch density limit at the longitudinal instability threshold, should be taken into account too; it should depend strongly on planned upgrade of the rf and feedback systems.

6. Differences between a linac-ring and other collider configurations

The luminosity formula given above applies to any kind of colliders, but the range of possible or simply best values attainable by each of the parameters is depending on the kind of accelerators. A linac-ring collider obviously has some in common with both a typical ring collider and a linear collider. As already pointed out, the quality of the electron beam must approach that required for a linear collider. The positron beam circulating in the ring should be affected as less as possible by the impinging linac beam. The strength of the beam-beam perturbation is usually characterized by the linear tune

shift parameter

$$\xi_i = \frac{n_b r_e \beta_i}{2\pi\gamma\sigma_i(\sigma_x+\sigma_z)} = \frac{n_b r_e \sqrt{\beta}_i}{2\pi\gamma\sqrt{k\epsilon_i}(\sigma_x+\sigma_z)}$$

where r_e is the classical radius of the electron, γ the relativistic factor of the stored beam and n_e the population of the impinging bunch. The experimental data from all the existing e^+e^- collider indicate that a bunch density limit corresponding to $\xi_{max} \approx 0.05$ cannot be exceeded. In a typical storage ring the luminosity is improved providing a low β in the interaction point and increasing the emittance so that larger n_b is usable at the maximum achievable ξ. This is of utmost importance when the storage ring is operated below the maximum energy where the natural decreasing of luminosity would be $\propto E^4$; this is indeed the case of CESR at $5.3\,GeV$. In the case of a linac ring collider the maximum average electron current providable by a linac is $\approx 10^2$ times lower than the stored positron current so the limit condition can be approached operating the ring at the lowest emittance. The ring parameters for a linac-ring collider are therefore more like to a synchrotron radiation source than to a standard ring collider. Since the goal luminosity is $\approx 10^2$ lower than that achieved at CESR the expected values of ξ are always well below the maximum value $\xi_{max} = 0.045$ measured in a variety of conditions [23].

Table 2. Parameter list of the superconducting linac.

Machine parameter		value	unit	Note
Energy	E_e	0.45	GeV	
Length	L	45	m	
Emittance	$\epsilon^L_{x,z}$	$1.0 \cdot 10^{-8}$	$m \cdot rad$	@ 1.0 GeV
Macropulse current	I_m	8	mA	
Particles/bunch	n_e	$1.8 \cdot 10^{10}$		7 bunches in 2.56 μs
Horiz. optical function	β_x	1.2	m	
Vert. optical function	β_z	$18 \cdot 10^{-3}$	m	
Beam size	σ_x	574	μm	
Beam size	σ_z	10	μm	
Bunch length	σ_y	3	mm	
Bunch frequency	f_b	3.333	MHz	
Macropulse duration	$T_o n$	1.0	ms	
Repetition rate	f_r	10	Hz	
Duty cycle	δ	0.01		

A lattice providing a very low β at the interaction region implies the presence of two focusing quadrupoles very close to IP to squeeze the beam waist. In our case operation at low emittance, while keeping constant $\sigma = \sqrt{\beta\epsilon}$, will allow a higher β and therefore a larger distance between the inner quadrupoles, giving more freedom in the design of the interaction region which is to be very peculiar due to the large energy ratio between electron and positron beams.

7. Possible improvements and alternatives

A number of potential or planned upgrades have been discussed during last years in papers presenting future development of CESR. Most of them are not directly of interest for a linac-ring collider in the configuration presented here since they imply very large number of bunches. However, every improvement in the feedback system and vacuum chamber impedance would reflect positively on this design, allowing operation at higher density bunches. The potentiality of different lattices must be also studied. A lattice providing $\beta_x = \beta_z$ and round beam at the interaction point is actively studied at CESR [24], to overcome the ξ_{max} limit. Of course it would be the most suited to match a round linac beam, relaxing the electron beam quality requirements.

Relevant changes with respect to the scenario considered here are possible when a large upgrade program will be completed to raise the storable current to 500 mA providing a luminosity $\sim 2 \cdot 10^{33}\, cm^{-2}s^{-1}$. Comparing this value with the luminosity required for our experiment the goal should be attainable with $I_{av} \leq 500\,\mu A$. This current can be obtained either by a 5 mA, 1% duty cycle sc linac, as outlined before, or even by a compact CW machine at lower current, such as a racetrack microtron. Although these machines usually provide $i_{av} < 100\,\mu A$, the recent operation of the TTF superconducting structure providing $8\,mA$ @ $10\,MeV$, and the planned operation of a CEBAF-like module providing $42\,MeV$ with energy recovery from the spent beam, indicate that multipass acceleration of current $\approx 500\,\mu A$ are conceivable.

8. Conclusion

Quite unexpected features, concerning the nucleon structure, have been found in measuring the nucleon time-like form factors. A new measurement is needed to confirm them.

The performances achieved in the past by CESR and those expected by a TTF-like linac allow to design an asymmetric, unconventional, linac-ring collider providing the luminosity needed for a real improvement in the measurement of the nucleon time-like form factors and of the total multihadronic cross section.

The boost in the laboratory frame of the outgoing particle will further improve the effectiveness of a new experiment.

Potential upgrading of both linac and storage ring performances should provide safe margins to reach the goal of a luminosity $\mathcal{L} = 10^{30} \div 10^{31}\ [cm^{-2}s^{-1}]$.

References

[1] M.N. Rosenbluth, Phys. rev. 79 (1950) 615;

[2] A.Zichichi, S.M.Berman, N.Cabibbo, R.Gatto, NC 24 (1962* 170;

[3] M.Castellano et al., Nuovo Cimento A14(1973)1; B.Delcourt et al., Phys.Lett. B86 (1979) 395; D.Bisello et al., Nucl.Phys. B224 (1983) 379; G.Bardin et al., Phys. Lett. B255(1991)154;

[4] FENICE coll. A.Antonelli et al. Phys. Lett. B334(1993)431;

[5] E760 coll. T.A. Armstrong et al. Phys.Rev.Lett. 70(1993)1212;

[6] A.A. Logunov, N. Van Hieu,I.T. Todorov Annals of Physics 31(1965)203;

[7] S.J. Brodsky, G.R. Farrar Phys.Rev. D11(1975)1309;

[8] W.Bilenky, I.Giunti and V.Wataghin, Zeit. fur Phys. C59(1993)459;

[9] FENICE coll. A.Antonelli et al. , Nucl. Instr. and Meth. A337(1993)34;

[10] FENICE coll. A.Antonelli et al. Phys. Lett. B313(1993)317;

[11] FENICE coll. A.Antonelli et al. Phys. Lett. B365(1996)427;

[12] M.E. Biagini, L. Cugusi, E. Pasqualucci Zeit. Phys. 52C(1991)631;

[13] A. Lung et al. Phys. Rev. Lett. 70(1993)718;

[14] H.W.Hammer et al., *Phys. Lett.* B367 (1996) 323; Z.Dziembowski and A.Szczurek *Phys. Lett.* B387 (1996) 875;

[15] V.L. Chernyak,I.R. Zhitnitski Nucl Phys. B246(1984)52;

[16] I.S. Shapiro Phys. Rep. 35(1978)129; A.M. Badalyan et al. Phys. Rep. 82(1982)31; G.C. Rossi, G. Veneziano Nucl. Phys. B123(1977)507;

[17] O.D.Dalkarov et al., Phys.Lett. B392(1997)229;

[18] S.Eidelman and F.Jegerlehner, PSI-PR-95-1 January 1995;

[19] F.Bergsma et al. Nucl. Instr. and Meth. A357(1995)243;

[20] D.L.Rubin, L.A.Schick, 'Single Interaction Point Operation * Proceeding of PAC 91 vol.1 (1991) 144;

[21] TESLA Test Facility - Conceptual Design Report, TESLA Report 95-1, DESY 1995;

[22] G.R.Neil et al., Nucl. Instr. and Meth. A358 (1995) 159;

[23] L.A.Schick,D.L.Rubin, 'Beam-beam Performances as a Fun* Proceeding of PAC 91 vol.1 (1991) 470;

[24] P.Bagley et al., 'Nearly equal β^* at CESR', Proceeding of PAC 91 vol.1 (1991) 467;